Clin Oral Invest (2016) 20:2211–2220
DOI 10.1007/s00784-016-1734-2

ORIGINAL ARTICLE

Mechanical properties of bone tissues surrounding dental implant systems with different treatments and healing periods

Do-Gyoon Kim[1] · Hyun-Jung Kwon[1] · Yong-Hoon Jeong[1] · Erin Kosel[1] · Damian J. Lee[2] · Jung-Suk Han[3] · Hye-Lee Kim[3] · Dae-Joon Kim[4]

Received: 18 November 2014 / Accepted: 21 January 2016 / Published online: 2 February 2016

Abstract
Objectives The objective of the current study was to examine whether the nanoindentation parameters can assess the alteration of bone quality resulting from different degrees of bone remodeling between bone tissue ages around the dental implant interface with different treatments and healing periods.
Materials and methods Dental implants were placed in mandibles of six male dogs. Treatment groups included: resorbable blast media-treated titanium (Ti) implants, alumina-blasted zirconia implants (ATZ), alumina-blasted zirconia implants applied with demineralized bone matrix (ATZ-D), and alumina-blasted zirconia implants applied with rhBMP-2 (ATZ-B). Nanoindentation modulus (E), hardness (H), viscosity (η), and viscoelastic creep (Creep/P_{max}) were measured for new and old bone tissues adjacent to the implants at 3 and 6 weeks of post-implantation. A total of 945 indentations were conducted for 32 implant systems.
Results Significantly lower E, H, and η but higher Creep/P_{max} were measured for new bone tissues than old bone tissues, independent of treatments at both healing periods ($p < 0.001$). All nanoindentation parameters were not significantly different between healing periods ($p > 0.568$). ATZ-D and ATZ-B implants had the stiffer slope of correlation between E and Creep/P_{max} of the new bone tissue than Ti implant ($p < 0.039$).
Conclusions Current results indicated that, in addition to elastic modulus and plastic hardness, measurement of viscoelastic properties of bone tissue surrounding the implant can provide more detailed information to understand mechanical behavior of an implant system.
Clinical relevance Ability of energy absorption in the interfacial bone tissue can play a significant role in the long-term success of a dental implant system.

Keywords Interfacial bone quality · Nanoindentation · Implant interface · Bone morphogenetic protein-2 · Bone remodeling

Introduction

Mechanical stability of a dental implant system is a critical factor in maintaining its high success rate during post-implantation healing and under functional masticatory loading [1–6]. Bone tissue surrounding the implant is inevitably damaged in the intensive surgical process of implantation. Active bone remodeling triggered by the surgical damage removes the pre-existing bone tissue and forms new bone tissue adjacent to the implant during post-implantation healing [4, 7]. Investigations on bone around dental implants retrieved from patients after a few weeks to 20 years or more in function indicated that active interfacial bone remodeling continued up to 5 years as stimulated by masticatory loading following post-implantation healing [6, 8]. It has been well accepted that the active bone remodeling alters bone

✉ Do-Gyoon Kim
kim.2508@osu.edu

[1] Division of Orthodontics, College of Dentistry, The Ohio State University, 4088 Postle Hall, 305 W. 12th Ave, Columbus, OH 43210, USA

[2] Division of Restorative Sciences and Prosthodontics, College of Dentistry, The Ohio State University, Columbus, OH 43210, USA

[3] Prosthodontics, Seoul National University, Seoul, South Korea

[4] Advanced Materials Engineering, Sejong University, Seoul, South Korea

quantity (bone area and bone-implant contact) and quality that can be determined by contents and distribution of collagen and mineral components of bone tissue around the implant, influencing the mechanical stability of implant system [4, 8–13].

It has been indicated that many factors including implant materials and bone growth agent treatment can alter quantity and quality of the regenerated bone tissue at the implant interface. For example, zirconium implants produced higher or comparable bone quantity adjacent to the implant as commercially pure titanium implants that have been most widely used in clinical practice [7, 14, 15]. It was also observed that the implant systems treated with demineralized bone matrix (DBM) and bone morphogenetic protein (BMP) have an effect on bone regeneration surrounding the implant [7, 16–19]. On the other hand, degree of tissue mineralization, as an indicator of bone quality, revealed strong correlations with the mechanical properties of bone [20–24]. As the newly formed bone tissue is not fully mineralized, the mechanical properties of new bone tissue resulting from the active bone remodeling adjacent to the implant are anticipated to be different from those of more mineralized, pre-existing old bone tissue away from the implant. However, there is a lack of studies that directly examined the tissue level properties of bone surrounding the implant because traditional mechanical testing devices were not able to precisely characterize the interfacial bone at the tissue level.

Nanoindentation has been widely utilized to measure mechanical properties of bone tissue at the submicron level [25, 26]. This technique has been also utilized to assess the bone quality at the narrow bone region around the implant interface [6, 11, 12]. These studies focused on assessment of the elastic modulus and hardness as the conventional parameters that are determined mostly by tissue mineral contents at the indentation site of bone. Recently, it was shown that time-dependent viscoelastic properties (viscosity and viscoelastic creep of bone tissue) can also be measured at the same indentation site and have significantly correlations with the elastic modulus and plastic hardness [27–29]. Collagen components, which are the main materials of bone tissue, control the viscoelastic properties [13, 21, 27]. Collagen consists of protein fibrils that show time-dependent deformation under loading. Minerals progressively arrange in collagen fibrils during the process of bone tissue mineralization determining the mechanical integrity of the mineral-collagen composite. As such, the alteration of bone tissue composition resulting from bone remodeling likely changes the combination of elastic, plastic, and viscoelastic characteristics of bone tissue. However, the viscoelastic property of bone around the implant has not been fully investigated.

Based on the recent findings, we hypothesized that the measures of nanoindentation parameters can distinguish differences of peri-implant bone quality between implant systems, which, in addition to bone quantity, can play an important role in determining mechanical stability of an implant system. Thus, the objective of the current study was to examine whether the nanoindentation parameters can assess alteration of bone quality resulting from different degrees of bone remodeling between bone tissue ages around the dental implant interface with different treatments and healing periods.

Materials and methods

Specimen preparation

Six beagle dogs (10 to 15 kg) were obtained following experimental protocol approval by the Institutional Animal Care and Use Committee (IACUC approval number: SNU-090502-2) of School of Dentistry, Seoul National University, Korea. All mandibular premolars and first molars were extracted. After a healing period of 12 weeks, four groups of implant system were placed as described in Table 1. Oxytetracycline hydrochloride (Merck, Amsterdam, The Netherlands; 20 mg/kg SQ), xylenol orange (Sigma, Zwijdrecht, The Netherlands; 90 mg/kg SQ), and calcein blue (Sigma; 90 mg/kg SQ) were administered at week 2, 4, and 5 after implant installation in order to label newly formed bone tissues at the corresponding weeks. Three dogs were sacrificed for each week 3 and 6 after implantation. Constructs including implants and adjacent alveolar bone were dissected and immediately fixed in 4 % neutral formaldehyde. Then, the constructs were embedded in light-curing resin (Technovit 7200 VLC; Kultzer, Wehrheim, Germany) and sectioned in the buccolingual direction using cutting–grinding technique (EXAKT Apparatebau, Norderstedt, Germany) up to a thickness of approximately 50 μm to expose the bone-implant interface (Fig. 1). The sectioned specimens were further polished with 1 μm diamond paste using a low-speed polisher for nanoindentation. Quality of the polished surfaces

Table 1 Description of the implant interfaces

Interfaces	Description
Ti	Titanium implant
ATZ-N	Alumina-toughened yttria and niobia co-doped tetragonal zirconia polycrystalline (ATZ) implant
ATZ-D	ATZ implant with demineralized bone matrix (DBM) gel
ATZ-B	ATZ implant with recombinant human bone morphogenetic protein-2 (rhBMP-2) in DBM gel

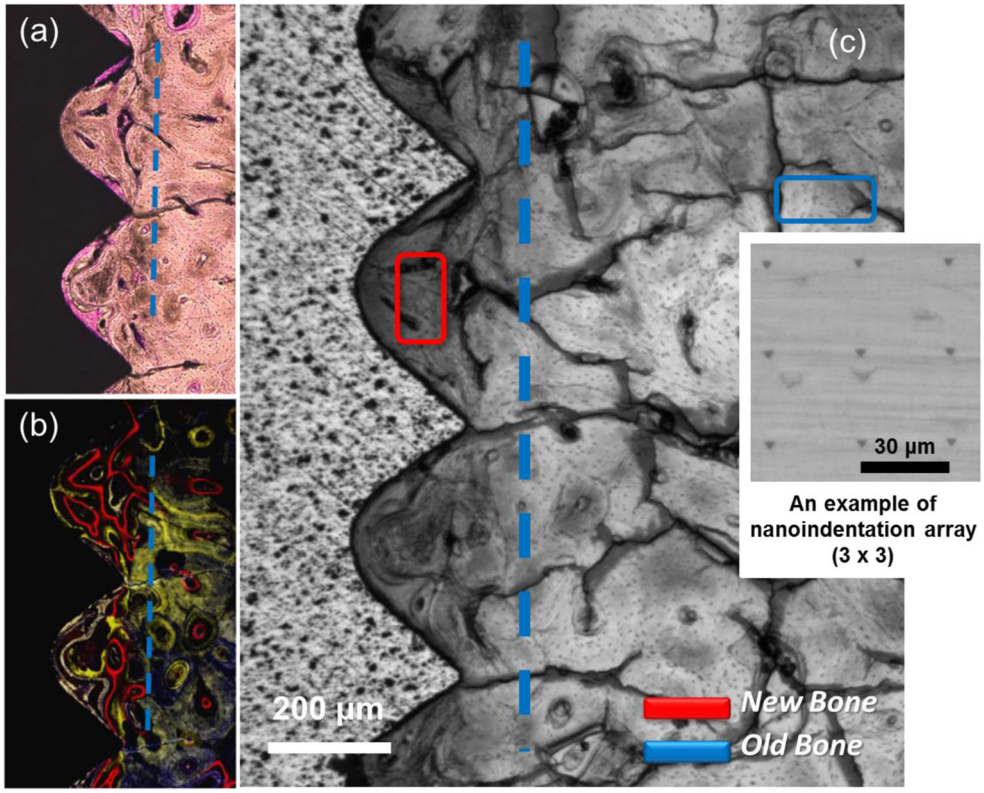

Fig. 1 Images at the bone-implant interface (ATZ-B at week 6) by comparing between **a** histologic (hematoxylin and eosin stain), **b** fluorescent, and **c** nanoindentation microscopic images. The *borderlines* (*blue dotted line*) between new and old bone tissues were clearly identified. The dimension of indentation sites is also shown for estimation

was confirmed by investigation under a light microscope.

The polished bone-implant interface specimens were mounted on a nanoindenter (Nano-XP, MTS, Oakridge, TN). Indentation regions were determined by comparing between histologic and nanoindenter microscopic images (Fig. 1). Newly formed bone tissues (New) adjacent the implant were identified by hematoxylin and eosin staining and fluorescent bone markers including oxytetracycline (yellow), xylenol orange (red), and calcein blue (blue).

Nanoindentation

In this study, nanoindentation was utilized to measure elastic modulus, plastic hardness, viscosity, and viscoelastic creep, which represent the capacity to resist elastic, plastic, and time-dependent viscous deformation and to sustain viscous deformation, respectively. Thus, the viscosity and viscoelastic creep have a reverse trend. Indentations were conducted under load control with the corresponding displacement rate of 10 nm/s up to indentation depth equivalent to 500 nm (Fig. 2).

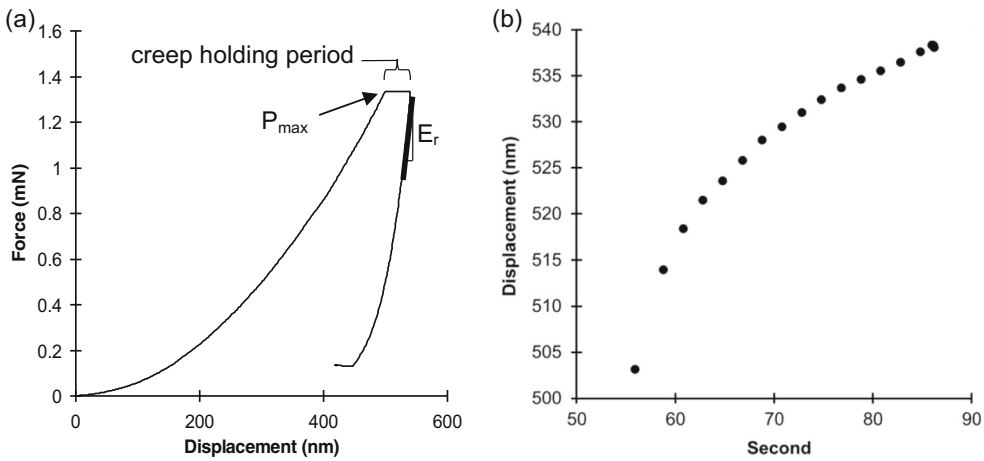

Fig. 2 **a** A typical nanoindentation curve and **b** creep during the holding period

A plastic hardness was obtained by the conventional Eq. 1 [30].

$$H = \frac{P_{max}}{A} \quad (1)$$

where P_{max} is the peak indenting load and A is the indenter contact area (A).

A constant peak loading produces a viscoelastic displacement (creep) during the 30-s hold period (Fig. 2b). Voigt model (Eq. 2) fits the displacement-time curve of creep.

$$h^2(t) = \frac{\pi}{2} P_{max} \cot\alpha \left[\frac{1}{E_2}\left(1 - e^{-tE_2/\eta}\right)\right] \quad (2)$$

where $h(t)$ is a time function of creep (nm), α is 65.27° as the face angle of the Berkovich indenter [31], and E_2 is an elastic component (GPa). Thus, the E_2 and η (viscosity) (GPaS) can be computed by the creep-time curve fitting. The Eq. 2 shows the reverse terms between the viscosity and viscoelastic creep. The applied peak load corresponding to the same loading depth (500 nm) varied between indentation sites because the intrinsic material properties of bone tissue are not homogeneous. In order to compare the effects of the intrinsic bone properties on creep independent of the different loading levels between indentation sites, it was valid to normalize the amount of creep by the peak load (Creep/P_{max}).

After the 30-s hold period, the indenter was unloaded with the same corresponding displacement rate of 10 nm/s. Nanoindentation elastic modulus (E) was computed using the conventional Eq. 3 [30].

$$\frac{1}{E_r} = \frac{(1-\nu_s^2)}{E_s} + \frac{(1-\nu_i^2)}{E_i} \quad (3)$$

The slope of unloading displacement-force curve was used to obtain E_r (reduced modulus). For the diamond Berkovich indenter, values of E_i = 1141 GPa and poisson's ratio (ν_i) = 0.07 are typically used. As ν_s for bone was assumed to be 0.3 following a previous study [32], the elastic modulus (E_s) of bone tissue specimen could be computed.

Statistical analysis

A total of 32 implant sites (4 for each Ti, ATZ-N, ATZ-D, and ATZ-B at week 3 and 6) were analyzed, only if its nanoindentation elastic modulus value was higher than 5 GPa to confirm mineralized bone tissues as measured in many nanoindentation studies for bone tissue obtained from various animals and human [21, 25, 32, 33]. In addition, measures containing errors in the process of searching for indentation surface and statistical outliers were removed as indicated in the previous studies [28, 34], Thus, the nanoindentation data obtained from a total

Table 2 Measures of nanoindentation parameters (E; elastic modulus, H; hardness, η; viscosity, and Creep/P_{max}; normalized creep) for the bone tissue ages (newly formed (New) and pre-existing old (Old) bone tissues) of four bone-implant interfaces (Ti, ATZ-N, ATZ-D, and ATZ-B) at week 3 and 6 after implantation

Groups	Weeks	Regions	E (GPa)	H (GPa)	η (GPaS)	Creep/P_{max} (nm/mN)
Ti	3	New	11.191 ± 3.269	0.457 ± 0.266	27,199.706 ± 11,516.740	16.955 ± 5.403
		Old	16.428 ± 2.269	0.648 ± 0.072	43,561.074 ± 6665.778	9.259 ± 1.940
	6	New	11.295 ± 0.837	0.411 ± 0.061	21,362.019 ± 3399.218	18.470 ± 3.084
		Old	15.143 ± 2.395	0.511 ± 0.087	32,831.966 ± 6488.893	12.350 ± 2.295
ATZ-N	3	New	12.411 ± 1.521	0.466 ± 0.069	27,194.189 ± 6694.703	14.847 ± 3.041
		Old	20.356 ± 1.396	0.784 ± 0.057	52,011.964 ± 3213.343	7.413 ± 0.777
	6	New	11.801 ± 1.679	0.436 ± 0.018	23,214.163 ± 965.535	15.686 ± 0.750
		Old	13.055 ± 4.578	0.484 ± 0.043	28,524.366 ± 5955.835	13.889 ± 2.214
ATZ-D	3	New	10.235 ± 0.744	0.349 ± 0.063	18,155.151 ± 4005.543	20.752 ± 4.431
		Old	18.031 ± 1.813	0.629 ± 0.043	37,695.012 ± 2758.584	9.530 ± 0.604
	6	New	11.420 ± 2.063	0.409 ± 0.069	22,398.314 ± 3594.587	16.674 ± 2.903
		Old	14.450 ± 5.063	0.528 ± 0.202	30,251.161 ± 13,898.564	15.013 ± 9.497
ATZ- B	3	New	11.170 ± 1.472	0.390 ± 0.090	20,792.378 ± 5960.974	18.755 ± 4.726
		Old	18.410 ± 3.893	0.729 ± 0.112	47,895.024 ± 7237.547	8.072 ± 1.695
	6	New	11.751 ± 2.227	0.410 ± 0.093	21,290.677 ± 6649.207	17.929 ± 5.611
		Old	15.559 ± 3.501	0.655 ± 0.125	39,537.787 ± 8410.914	9.756 ± 2.630

Data are presented as mean ± standard deviation for each parameter

number of 945 indents, 472 indents from week 3 specimens (221 from the newly formed bone tissues (New) and 251 from the pre-existing old bone tissues (Old)) and 473 indents from week 6 specimens (235 from the New group and 238 from the Old group), were included for the current analysis.

Mixed model repeated measures analysis of variance (SPSS, IBM), followed by Sidax post hoc test, was conducted to analyze the effects of the healing periods and implants on differences of the nanoindentation parameters (E; elastic modulus, H; plastic hardness, η; viscosity, and Creep/P_{max}; viscoelastic normalized creep) between the New and Old groups. Then, multivariate analysis of variance was utilized to compare the nanoindentation parameters between the effective factors. Correlations of the elastic modulus with other nanoindentation parameters were examined using Pearson's correlation tests. Analysis of covariance (ANCOVA) was used to investigate whether those correlations are different between the tissue age groups (New and Old) and the new bone tissue of implant treatment groups (Ti, ATZ-N, ATZ-D, and ATZ-B), which is anticipated to have active bone remodeling resulting from those treatments. Significance was set at $p < 0.05$.

Results

A clear border between the pre-existing bone and the newly formed bone was observed in histologic, fluorescent, and nanoindentation microscopic images (blue dotted lines, Fig. 1). The indentation sites were identified by comparing between those images that showed the relatively new bone tissues within the borderline approximately between the implant threads (New) from the relatively old pre-existing bone tissues away from the border (Old) (Fig. 1). A typical indentation curve was obtained for all indent sites (Fig. 2a). Excellent fittings were observed for all indentation creep curves using the Voigt model ($r^2 > 0.97$, $p < 0.001$).

The new bone tissue group had significantly lower mean values of elastic modulus (E), plastic hardness (H), and viscosity (η) but higher mean values of viscoelastic normalized creep (Creep/P_{max}) than the old bone tissue group ($p < 0.001$) (Table 2). The healing periods (3 and 6 weeks) had significant effects on the differences of the mean values of all nanoindentation parameters between new and old tissue groups ($p < 0.012$), while the implant groups (Ti, ATZ-N, ATZ-D, and ATZ-B) did not have any effect ($p > 0.119$). The new bone tissue group did not have significantly different mean values of all nanoindentation parameters between the healing periods

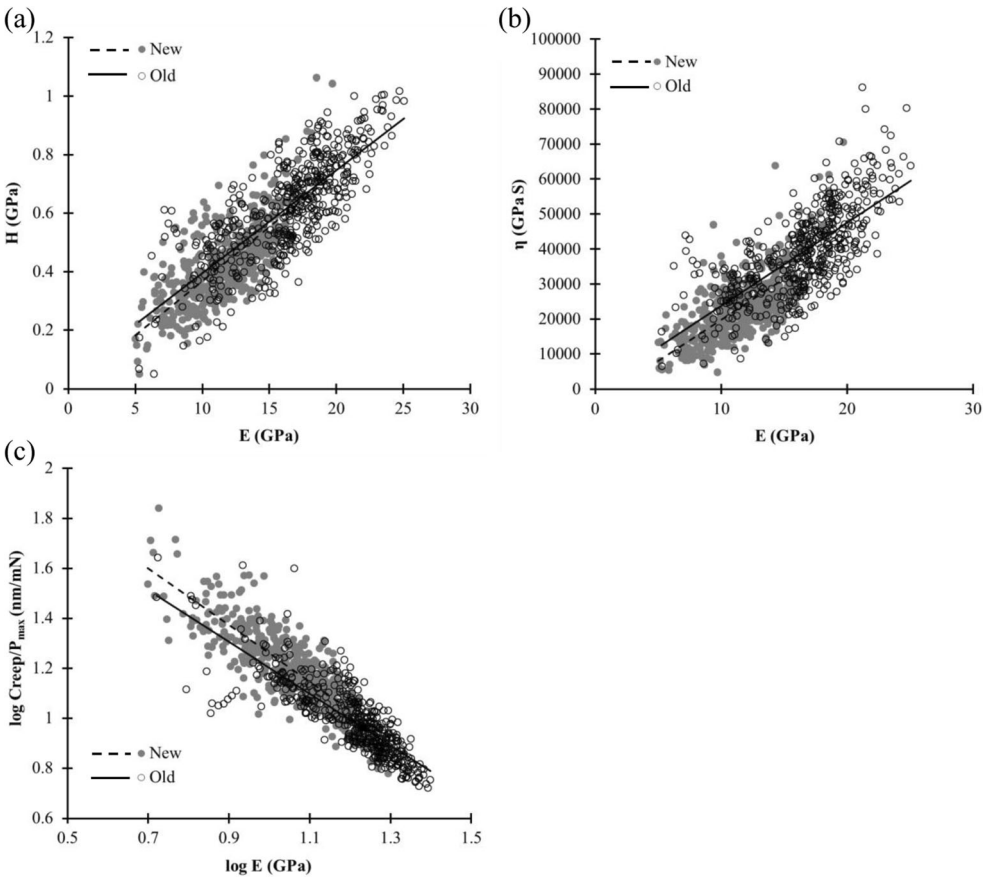

Fig. 3 Significant correlations of elastic modulus (E) with **a** plastic hardness (H), **b** viscosity (η), and **c** normalized creep (Creep/P_{max}) for the New and Old groups

Table 3 Correlations of elastic modulus (E) with plastic hardness (H), viscosity (η), and viscoelastic normalized creep (Creep/P_{max}) for interfacial bone tissue ages (New, $n = 456$ and Old, $n = 489$) and for the bone-implant interfaces of New group. All correlations were significant ($p < 0.001$)

X	Y	Group		Correlations	r
E	H	New		$Y = 0.037X - 0.004$	0.744
		Old		$Y = 0.035X + 0.044$	0.781
		New	Ti	$Y = 0.034X + 0.047$	0.699
			ATZ-N	$Y = 0.040X - 0.042$	0.735
			ATZ-D	$Y = 0.040X - 0.047$	0.792
			ATZ-B	$Y = 0.043X - 0.085$	0.850
E	η	New		$Y = 2359.325X - 3839.677$	0.703
		Old		$Y = 2378.659X - 29.786$	0.717
		New	Ti	$Y = 2189.525X - 541.926$	0.676
			ATZ-N	$Y = 2693.674X - 7577.598$	0.665
			ATZ-D	$Y = 2473.046X - 6279.078$	0.772
			ATZ-B	$Y = 2391.950X - 6102.327$	0.805
log E	log Creep/P_{max}	New		$Y = -1.132X + 2.391$	0.829
		Old		$Y = -1.035X + 2.236$	0.828
		New	Ti	$Y = -1.023X + 2.263$	0.812
			ATZ-N	$Y = -1.190X + 2.450$	0.770
			ATZ-D	$Y = -1.245X + 2.523$	0.853
			ATZ-B	$Y = -1.320X + 2.610$	0.914

($p > 0.568$), while the old tissue group significantly changed during healing periods ($p < 0.004$).

The elastic modulus (E) had strong positive correlations with plastic hardness (H) and viscosity (η), but a strong negative correlation with viscoelastic normalized creep (Creep/P_{max}) for the pooled groups ($r > 0.807$, $p < 0.001$) (Fig. 3 and Table 3). The new bone tissue group had a significantly stiffer correlation slope of E with Creep/P_{max} than the old bone tissue group (ANCOVA, $p = 0.043$), while those with other parameters were not significantly different (ANCOVA, $p > 0.351$) (Fig. 3). The correlation slope of E with Creep/P_{max} for the new bone tissue at the Ti implant interface was significantly different from those at the ATZ-D and ATZ-B implant interfaces (ANCOVA, $p < 0.039$), while those with other parameters were not significantly different between the implant interfaces (ANCOVA, $p > 0.108$) (Fig. 4).

Discussion

The lower elastic modulus (E), plastic hardness (H), viscosity (η), and higher normalized creep (Creep/P_{max}) of the newly formed bone tissue provide lower capacity to resist elastic, plastic, and time-dependent viscous deformation but higher ability to absorb energy in sustaining viscous deformation than those of the pre-existing old bone tissue. This can help the implant interface to bear constant static occlusion and time-dependent dynamic impact of masticatory loading. These compliant properties of the newly formed bone tissue adjacent to the implant consistently maintained at the longer healing period, while those of the pre-existing old bone tissue away from the implant changed. This observation indicates that the interfacial bone continuously remodeled during the healing periods, producing the less mineralized new bone tissue. The newly formed interfacial bone tissue had the stiffer correlation slope of E with Creep/P_{max} than the pre-existing old bone tissue. Similarly, the new bone tissue at ATZ implant interfaces with DBM and rhBMP-2 had the stiffer slope of correlation between E and Creep/P_{max} than new bone tissue at the untreated Ti implant interface. These results indicate that, given the same level of elastic modulus, the interfacial bone tissues of DBM and rhBMP-2 treated implant systems could provide higher ability of energy absorption than those of untreated Ti implant system as occurred at the new interfacial bone region than at the old pre-existing bone region.

The newly formed bone tissues around the ATZ-N interface had the comparable values of mechanical properties with those at the Ti interface at each healing period. This finding is consistent with the previous observation that showed the similar histological measures of the ATZ-N as those of Ti implant systems [7]. These results suggested that the implant materials may not have a substantial effect on determining the quantity and quality of interfacial bone at the early healing stage.

The mechanical properties of bone tissue around the dental implant have been measured focusing on its modulus and hardness [10–12]. As bone is a viscoelastic material, it shows

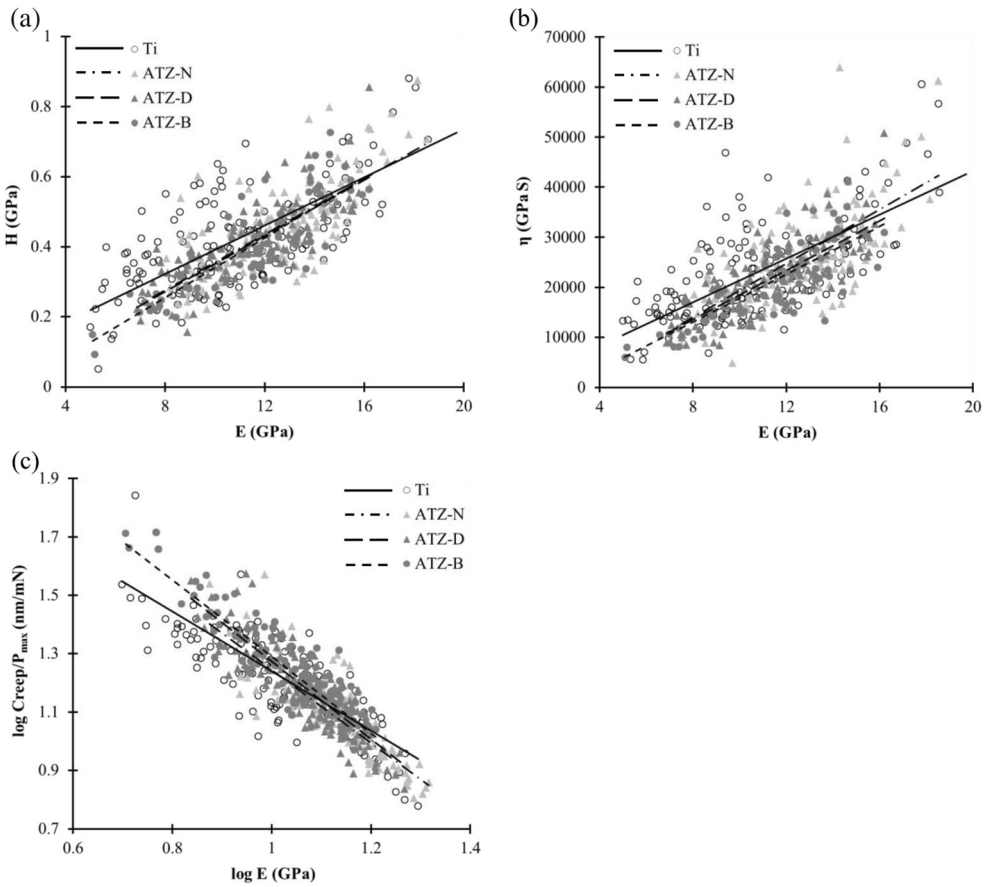

Fig. 4 Significant correlations of elastic modulus (E) with **a** plastic hardness (H), **b** viscosity (η), and **c** normalized creep (Creep/P_{max}) for the implant interfaces of New group

time-dependent response in absorbing and dissipating energy under mechanical loading [28, 35, 36]. Recently, the traditional viscoelastic Voigt model has been introduced for nanoindentation-based measurement of viscoelastic properties of bone tissue [27, 28]. Following these previous works, the current study demonstrated that the viscosity and viscoelastic creep can be successfully assessed along with the elastic modulus and plastic hardness by a cycle of indentation at the same site of bone tissue around the implant interface during healing periods. It should be noted that the viscosity accounts for resistance against viscous deformation and the viscoelastic creep is determined depending on the ability of a material to sustain viscous deformation in a given time period. As such, the reverse behavior is usually observed between those properties as assessed in the current study.

It has been well observed that damages to bone at the process of vigorous implantation surgery stimulate active bone remodeling adjacent to the implant [4, 9]. The damaged bone tissue is resorbed and new bone tissue is formed and then continuously matured by a long-term mineralization. As such, the newly formed bone tissue has less mineral than the pre-existing old bone tissue [24]. Many studies measured lower nanoindentation modulus, hardness, and viscosity but more viscoelastic properties at the less mineralized bone tissue than the more mineralized bone tissue [21–23, 27, 28, 37, 38]. It was indicated that the lower viscosity but higher creep measured in the less mineralized bone tissue help to dissipate and absorb loading energy compromising increase in the risk of tissue damage due to its lower modulus and hardness [28, 39]. These previous observations supported the current findings that less mineralization of the newly formed bone tissue adjacent to the implant provided more viscoelastic properties than the pre-existing old bone tissue away from the implant. During normal mastication, a high impact energy from masticatory loading on teeth is absorbed through the highly viscoelastic periodontal ligament [5, 40, 41]. For the successfully osseointegrated dental implant system, the masticatory loading directly transmitted to the adjacent interfacial bone should be efficiently absorbed by the newly formed bone tissue around the dental implant interface. Previous studies using dental implant system retrieved from human patients have indicated that active bone remodeling is continuously stimulated by dynamic masticatory loading for years following post-implantation healing periods producing new bone tissues around the implant [6, 8, 42]. Those retrieved implant systems also maintain a high bone-implant contact percentage. Taken together, these findings can provide an insight into how the less mineralized new bone tissue resulting from the active

bone remodeling adjacent to the implant is able to bear the high impact energy of masticatory loading directly transmitted from the implant without the periodontal ligament. This energy absorption capability of the interfacial bone tissue surrounding the implant likely plays a significant role in the long-term success of a dental implant system.

It was observed that the nanoindentation modulus and hardness have strong positive relationships with degree of mineralization [22, 23]. The current results showed that the correlation slopes of modulus with the hardness and viscosity were the same between the new and old interfacial bone tissues. These findings indicate that the same mechanism of tissue mineralization controls the plastic hardness and viscosity of the new and old bone tissues. On the other hand, the normalized viscoelastic creep of the new bone tissue had stiffer slopes of correlation with the elastic modulus than that of the old bone tissue. This finding indicates that the less mineralized new interfacial bone can obtain a better viscoelastic mechanical stability of the implant system by providing more energy absorption even if the same level of elastic deformation is engaged, compared to the more mineralized old bone tissue.

No significant effects of DBM and rhBMP-2 treatments on the absolute values of nanoindentation parameters were found. In contrast, the zirconia implant with DBM (ATZ-D) and rhBMP-2 (ATZ-B) had significantly stiffer correlation slopes between modulus and creep of the new bone tissue than Ti implant. Again, this result indicates that the ATZ-D and ATZ-B implant systems would have more advantage to absorb the loading energy than the Ti implant system when the same level of E, which is proportion to tissue mineralization, exists between those implant systems. This observation suggests that there may be other mechanism responsible for controlling these treatment-dependent correlations than the different levels of tissue mineralization. It was postulated that the progressive arrangement of minerals in collagen fibrils, which is organized during the process of bone tissue mineralization, is responsible for the mechanical integrity of mineral/collagen composite [43, 44]. More bone turnover stimulated by the DBM or rhBMP-2 could produce more immature bone tissue that consists of less organized bone mineral and collagen while maintaining the same level of mineralization. Further studies are needed to clarify this mechanism.

A limitation of the current study was that the bone-implant specimens were not fresh but dry and embalmed to prepare the slices for histology and nanoindentation. This is an inevitable step to prevent decay of bone tissue during a long curing time of resin to hold the bone-implant construct for dissection and grinding. Thus, all of the previous studies provided valuable results based on nanoindentation for the dry embalmed bone-implant construct embedded in resin [11, 12, 45]. However, it was indicated that the drying and embalming could alter the measures of modulus, hardness, and viscoelastic properties of bone tissue [33, 46]. The current value of modulus was measured at the comparable range of the modulus (10.70 to 16.54 GPa) measured from the previous study that conducted nanoindentation on fresh mandibular alveolar bone specimens of dog [32]. In addition, the significant correlations of modulus with hardness, viscosity, and normalized creep found in the current study were consistent with those in the previous nanoindentation study using the fresh dog femur specimens [28]. These observations can validate the current findings.

In conclusion, the nanoindentation parameters including the elastic modulus, plastic hardness, viscosity, and viscoelastic creep were successfully assessed by a cycle of indentation at the same site of bone tissue surrounding the implant. The active bone remodeling adjacent to the implant regenerates the new bone tissue that has lower ability to resist elastic, plastic, and viscous deformation but higher viscoelastic capacity to absorb deformation energy than the old pre-existing bone tissue. Continuous remodeling at the new bone tissue produces the same levels of nanoindentation measures between different durations of post-implantation healing and treatments. However, the viscoelastic mechanical response at the same level of elastic modulus varied between the new peri-implant bone tissues with different treatments. The current findings suggest that, in addition to the conventional elastic and plastic properties, viscoelastic properties of bone tissue surrounding the implant should be considered as important mechanical characteristics to understand the working mechanism of a successful implant system.

Acknowledgments The project described was, in part, supported by American Association of Orthodontists Foundation Award (Kim, D-G). The authors would like to thank Kathy L. Elias and Cheol-Woo Park who helped collecting data.

Compliance with ethical standards This article does not contain any studies with human participants or animals performed by any of the authors.

Conflict of interest The authors declare that they have no competing interests.

Informed consent For this type of study, formal consent is not required.

References

1. Isidor F (2006) Influence of forces on peri-implant bone. Clin Oral Implants Res 17(Supplement 2):8–18. doi:10.1111/j.1600-0501.2006.01360.x
2. Hoshaw SJ, Brunski JB, Cochran GV (1994) Mechanical loading of Brånemark implants affects interfacial bone modeling and remodeling. Int J Oral Max Impl 9(3):345–360

3. Lin D, Li Q, Li W, Duckmanton N, Swain M (2010) Mandibular bone remodeling induced by dental implant. J Biomech 43(2):287–293. doi:10.1016/j.jbiomech.2009.08.024
4. Kim DG, Huja SS, Tee BC, Larsen PE, Kennedy KS, Chien HH, Lee JW, Wen HB (2013a) Bone ingrowth and initial stability of titanium and porous tantalum dental implants: a pilot canine study. Implant Dent 22(4):399–405. doi:10.1097/ID.0b013e31829b17b5
5. Brunski JB (1988) Biomaterials and biomechanics in dental implant design. The Int J Oral Max Impl 3(2):85–97
6. Baldassarri M, Bonfante E, Suzuki M, Marin C, Granato R, Tovar N, Coelho PG (2012) Mechanical properties of human bone surrounding plateau root form implants retrieved after 0.3–24 years of function. J Biomed Mater Res B Appl Biomater 100(7):2015–2021. doi:10.1002/jbm.b.32786
7. Lee BC, Yeo IS, Kim DJ, Lee JB, Kim SH, Han JS (2013) Bone formation around zirconia implants combined with rhBMP-2 gel in the canine mandible. Clin Oral Implants Res 24(12):1332–1338. doi:10.1111/clr.12004
8. Piattelli A, Artese L, Penitente E, Iaculli F, Degidi M, Mangano C, Shibli JA, Coelho PG, Perrotti V, Iezzi G (2014) Osteocyte density in the peri-implant bone of implants retrieved after different time periods (4 weeks to 27 years). J Biomed Mater Res B Appl Biomater 102(2):239–243. doi:10.1002/jbm.b.33000
9. Garetto LP, Chen J, Parr JA, Roberts WE (1995) Remodeling dynamics of bone supporting rigidly fixed titanium implants: a histomorphometric comparison in four species including humans. Implant Dent 4(4):235–243
10. Maimoun L, Brennan TC, Badoud I, Dubois-Ferriere V, Rizzoli R, Ammann P (2010) Strontium ranelate improves implant osseointegration. Bone 46(5):1436–1441. doi:10.1016/j.bone.2010.01.379
11. Anchieta RB, Baldassarri M, Guastaldi F, Tovar N, Janal MN, Gottlow J, Dard M, Jimbo R, Coelho PG (2013) Mechanical property assessment of bone healing around a titanium-zirconium alloy dental implant. Clin Implant Dent Relat Res. doi:10.1111/cid.12061
12. Jimbo R, Coelho PG, Bryington M, Baldassarri M, Tovar N, Currie F, Hayashi M, Janal MN, Andersson M, Ono D, Vandeweghe S, Wennerberg A (2012) Nano hydroxyapatite-coated implants improve bone nanomechanical properties. J Dent Res 91(12):1172–1177. doi:10.1177/0022034512463240
13. Morris MD, Mandair GS (2011) Raman assessment of bone quality. Clin Orthop Relat Res 469(8):2160–2169. doi:10.1007/s11999-010-1692-y
14. Gottlow J, Dard M, Kjellson F, Obrecht M, Sennerby L (2012) Evaluation of a new titanium-zirconium dental implant: a biomechanical and histological comparative study in the mini pig. Clin Implant Dent Relat Res 14(4):538–545. doi:10.1111/j.1708-8208.2010.00289.x
15. Shin D, Blanchard SB, Ito M, Chu TM (2011) Peripheral quantitative computer tomographic, histomorphometric, and removal torque analyses of two different non-coated implants in a rabbit model. Clin Oral Implants Res 22(3):242–250. doi:10.1111/j.1600-0501.2010.01980.x
16. Wikesjo UM, Huang YH, Xiropaidis AV, Sorensen RG, Rohrer MD, Prasad HS, Wozney JM, Hall J (2008) Bone formation at recombinant human bone morphogenetic protein-2-coated titanium implants in the posterior maxilla (type IV bone) in non-human primates. J Clin Periodontol 35(11):992–1000. doi:10.1111/j.1600-051X.2008.01322.x
17. Sykaras N, Triplett RG, Nunn ME, Iacopino AM, Opperman LA (2001) Effect of recombinant human bone morphogenetic protein-2 on bone regeneration and osseointegration of dental implants. Clin Oral Implants Res 12(4):339–349
18. Leknes KN, Yang J, Qahash M, Polimeni G, Susin C, Wikesjo UM (2012) Alveolar ridge augmentation using implants coated with recombinant human growth/differentiation factor-5 (rhGDF-5). radiographic observations. Clin Oral Implants Res 24(11):1185–1191. doi:10.1111/j.1600-0501.2012.02564.x
19. Schliephake H (2013) Clinical efficacy of growth factors to enhance tissue repair in oral and maxillofacial reconstruction: a systematic review. Clin Implant Dent Relat Res. doi:10.1111/cid.12114
20. Currey JD (1999) The design of mineralised hard tissues for their mechanical functions. J Exp Biol 202(Pt 23):3285–3294
21. Donnelly E, Boskey AL, Baker SP, van der Meulen MC (2010) Effects of tissue age on bone tissue material composition and nanomechanical properties in the rat cortex. J Biomed Mater Res A 92(3):1048–1056. doi:10.1002/jbm.a.32442
22. Mulder L, Koolstra JH, den Toonder JMJ, van Eijden TMGJ (2007) Intratrabecular distribution of tissues stiffness and mineralization in developing trabecular bone. Bone 41(2):256–265
23. Mulder L, Koolstra JH, den Toonder JM, van Eijden TM (2008) Relationship between tissue stiffness and degree of mineralization of developing trabecular bone. J Biomed Mater Res A 84(2):508–515
24. Ruffoni D, Fratzl P, Roschger P, Klaushofer K, Weinkamer R (2007) The bone mineralization density distribution as a fingerprint of the mineralization process. Bone 40(5):1308–1319
25. Hoffler CE, Guo XE, Zysset PK, Goldstein SA (2005) An application of nanoindentation technique to measure bone tissue lamellae properties. J Biomech Eng 127(7):1046–1053
26. Rho JY, Tsui TY, Pharr GM (1997) Elastic properties of human cortical and trabecular lamellar bone measured by nanoindentation. Biomaterials 18(20):1325–1330
27. Kim DG, Huja SS, Navalgund A, D'Atri A, Tee B, Reeder S, Ri Lee H (2013b) Effect of estrogen deficiency on regional variation of a viscoelastic tissue property of bone. J Biomech 46(1):110–115. doi:10.1016/j.jbiomech.2012.10.013
28. Kim DG, Huja SS, Lee HR, Tee BC, Hueni S (2010) Relationships of viscosity with contact hardness and modulus of bone matrix measured by nanoindentation. J Biomech Eng 132(2):024502. doi:10.1115/1.4000936
29. Kim DG, Elias K (2014) Handbook of nanomaterials properties. In: Bhushan B, Luo D, Schricker SR, Sigmund W, Zauscher S (eds) Elastic, viscoelastic, and fracture properties of bone tissue measured by nanoindentation. Springer, Berlin, pp. 1321–1341
30. Oliver WC, Pharr GM (2004) Measurement of hardness and elastic modulus by instrumented indentation: advances in understanding and refinements to methodology. J Mater Res 19(1):3–20. doi:10.1557/jmr.2004.19.1.3
31. Fischer-Cripps AC (2004) A simple phenomenological approach to nanoindentation creep. Mat Sci Eng A-Struct 385(1–2):74–82. doi:10.1016/j.msea.2004.04.070
32. Huja SS, Fernandez SA, Hill KJ, Gulati P (2007) Indentation modulus of the alveolar process in dogs. J Dent Res 86(3):237–241
33. Rho JY, Pharr GM (1999) Effects of drying on the mechanical properties of bovine femur measured by nanoindentation. J Mater Sci Mater Med 10(8):485–488
34. Hoffler CE, Moore KE, Kozloff K, Zysset PK, Brown MB, Goldstein SA (2000) Heterogeneity of bone lamellar-level elastic moduli. Bone 26(6):603–609
35. Lakes RS (1999) Viscoelastic solid. CRC Press, New York, p. 267
36. Kim DG, Navalgund AR, Tee BC, Noble GJ, Hart RT, Lee HR (2012) Increased variability of bone tissue mineral density resulting from estrogen deficiency influences creep behavior in a rat vertebral body. Bone 51(5):868–875. doi:10.1016/j.bone.2012.08.124
37. Donnelly E, Williams RM, Downs SA, Dickinson ME, Baker SP, van der Meulen MCH (2006) Quasistatic and dynamic nanomechanical properties of cancellous bone tissue relate to collagen content and organization. J Mater Res 21(8):2106–2117. doi:10.1557/Jmr.2006.0259
38. Isaksson H, Malkiewicz M, Nowak R, Helminen HJ, Jurvelin JS (2010a) Rabbit cortical bone tissue increases its elastic stiffness but

becomes less viscoelastic with age. Bone 47(6):1030–1038. doi:10.1016/j.bone.2010.08.015

39. Isaksson H, Nagao S, Malkiewicz M, Julkunen P, Nowak R, Jurvelin JS (2010b) Precision of nanoindentation protocols for measurement of viscoelasticity in cortical and trabecular bone. J Biomech 43(12):2410–2417. doi:10.1016/j.jbiomech.2010.04.017
40. Poiate IA, de Vasconcellos AB, de Santana RB, Poiate E (2009) Three-dimensional stress distribution in the human periodontal ligament in masticatory, parafunctional, and trauma loads: finite element analysis. J Periodontol 80(11):1859–1867. doi:10.1902/jop.2009.090220
41. Ona M, Wakabayashi N (2006) Influence of alveolar support on stress in periodontal structures. J Dent Res 85(12):1087–1091
42. Iezzi G, Degidi M, Shibli JA, Vantaggiato G, Piattelli A, Perrotti V (2013) Bone response to dental implants after a 3- to 10-year loading period: a histologic and histomorphometric report of four cases. Int J Periodontics Restorative Dent 33(6):755–761. doi:10.11607/prd.1257
43. Jager IL (2005) A model for the stability and creep of organic materials. J Biomech 38(7):1459–1467
44. Gupta HS, Krauss S, Kerschnitzki M, Karunaratne A, Dunlop JW, Barber AH, Boesecke P, Funari SS, Fratzl P (2013) Intrafibrillar plasticity through mineral/collagen sliding is the dominant mechanism for the extreme toughness of antler bone. J Mech Behav Biomed Mater 28:366–382. doi:10.1016/j.jmbbm.2013.03.020
45. Oyen ML, Ko CC (2007) Examination of local variations in viscous, elastic, and plastic indentation responses in healing bone. J Mater Sci Mater Med 18(4):623–628
46. Pathak S, Swadener JG, Kalidindi SR, Courtland HW, Jepsen KJ, Goldman HM (2011) Measuring the dynamic mechanical response of hydrated mouse bone by nanoindentation. J Mech Behav Biomed Mater 4(1):34–43. doi:10.1016/j.jmbbm.2010.09.002